© 2016. Published by The Company of Biologists Ltd | Development (2016) 143, 2689 doi:10.1242/dev.141515

CORRECTION

Regulation of cortical contractility and spindle positioning by the protein phosphatase 6 PPH-6 in one-cell stage *C. elegans* embryos

Katayoun Afshar, Michael E. Werner, Yu Chung Tse, Michael Glotzer and Pierre Gönczy

There was an error published in Development **137**, 237-247.

In Fig. 2D, owing to the PPH-6 film being inadvertently flipped during scanning, the two lanes labelled as input instead showed flowthrough. A revised Fig. 2 with the correct input samples in D is shown below. In addition, a note has been added to the end of the legend to clarify the lack of GFP-SAPS-1 signal in these input lanes.

This error does not affect the conclusions of this experiment or of the paper. The authors apologise to readers for this mistake.

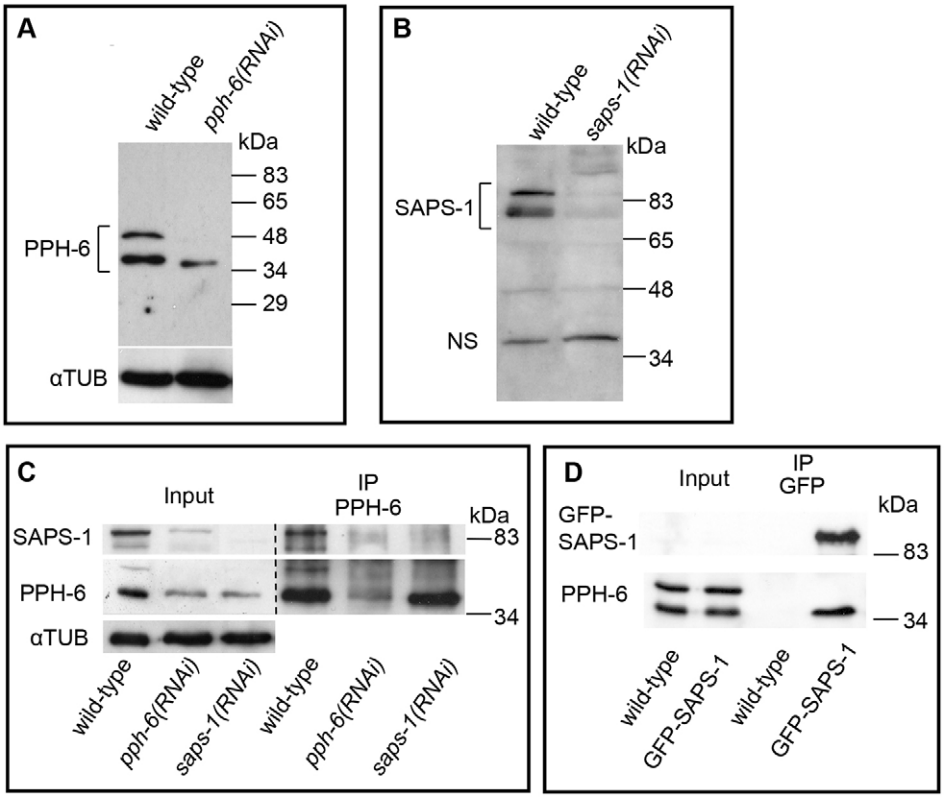

Fig. 2. PPH-6 and SAPS-1 associate *in vivo*. (A) Western blot analysis using PPH-6 antibodies on wild-type or *pph-6(RNAi)* embryonic extracts. The blot was reprobed with α-tubulin antibodies as a loading control (bottom). Note the presence of two species, with the lower one exhibiting the predicted molecular weight of PPH-6 (~37 kDa). Note also that the ratio between these two species varies among extracts (compare A with inputs in C). Similar variability is observed for SAPS-1 (B,C). The variation might be due to differences in the developmental stages of the embryos in the different preparations. (B) Western blot analysis of wild-type or *saps-1(RNAi)* embryonic extracts probed with SAPS-1 antibodies. Note presence of two major specific species, exhibiting the predicted molecular weight of the splice variants of SAPS-1 (~80 kDa and 87 kDa). A non-specific band (NS) served as a loading control. (C) Coimmunoprecipitation from wild-type, *pph-6(RNAi)* or *saps-1(RNAi)* embryonic extracts using PPH-6 antibodies. Western blots were probed with antibodies against PPH-6, SAPS-1 or α-tubulin, as indicated. In the second row, the input is exposed 10 times longer than the IP. Input/IP=1:50. In three independent experiments, we observed that PPH-6 antibodies retrieved more PPH-6 from the *saps-1(RNAi)* extract than from the *pph-6(RNAi)* extract, despite similar depletion levels of PPH-6. Perhaps PPH-6 not bound to SAPS-1 is more accessible to PPH-6 antibodies. (D) Extract from embryos expressing GFP-SAPS-1 or from wild-type embryos immunoprecipitated with GFP antibodies and analyzed by western blot with GFP or PPH-6 antibodies, as indicated. Note that only the PPH-6 species with the lower molecular weight co-immunoprecipitates with GFP-SAPS-1. Input/IP=1:50 (overall levels of GFP-SAPS-1 protein in the embryonic lysates are low, hence the lack of detection of GFP-SAPS-1 in the input lanes).

Development 137, 237-247 (2010) doi:10.1242/dev.042754

Regulation of cortical contractility and spindle positioning by the protein phosphatase 6 PPH-6 in one-cell stage *C. elegans* embryos

Katayoun Afshar[1], Michael E. Werner[2,†], Yu Chung Tse[2,*,†], Michael Glotzer[2,‡] and Pierre Gönczy[1,‡]

SUMMARY

Modulation of the microtubule and the actin cytoskeleton is crucial for proper cell division. Protein phosphorylation is known to be an important regulatory mechanism modulating these cytoskeletal networks. By contrast, there is a relative paucity of information regarding how protein phosphatases contribute to such modulation. Here, we characterize the requirements for protein phosphatase PPH-6 and its associated subunit SAPS-1 in one-cell stage *C. elegans* embryos. We establish that the complex of PPH-6 and SAPS-1 (PPH-6/SAPS-1) is required for contractility of the actomyosin network and proper spindle positioning. Our analysis demonstrates that PPH-6/SAPS-1 regulates the organization of cortical non-muscle myosin II (NMY-2). Accordingly, we uncover that PPH-6/SAPS-1 contributes to cytokinesis by stimulating actomyosin contractility. Furthermore, we demonstrate that PPH-6/SAPS-1 is required for the proper generation of pulling forces on spindle poles during anaphase. Our results indicate that this requirement is distinct from the role in organizing the cortical actomyosin network. Instead, we uncover that PPH-6/SAPS-1 contributes to the cortical localization of two positive regulators of pulling forces, GPR-1/2 and LIN-5. Our findings provide the first insights into the role of a member of the PP6 family of phosphatases in metazoan development.

KEY WORDS: Cytoskeleton, Asymmetric cell division, Cortical pulling forces, *C. elegans*, Actomyosin network

INTRODUCTION

Proper cell division requires the precise spatial and temporal coordination of processes such as spindle assembly, chromosome segregation, spindle positioning and cytokinesis. Alterations in these processes can result in genome instability and deleterious consequences for the organism. A variety of experimental approaches have uncovered proteins and pathways that are essential for cell division. Despite such progress, the underlying mechanisms remain incompletely understood, in part because components that may play important but non-essential roles have proven more challenging to identify, in particular in a developing organism.

Changes in cytoskeletal organization are critical for proper cell division. To this end, the microtubule and the actomyosin cytoskeleton are modulated notably through phosphorylation by a vast array of protein kinases. For example, the Aurora and Polo families of Ser/Thr kinases regulate microtubule nucleation, spindle assembly, chromosome segregation and cytokinesis by phosphorylating crucial centrosomal components, motor proteins and regulators of the RhoA GTPase (reviewed by Archambault and Glover, 2009; Taylor and Peters, 2008). Similarly, the Rho-associated kinase (ROCK) phosphorylates the regulatory light chain of non-muscle myosin II, thus promoting its motor activity and contractility of the actomyosin network during cytokinesis (reviewed by Matsumura, 2005; Piekny et al., 2005). Given that phosphorylation events must be tightly regulated in time and space, the action of kinases must be counteracted by that of phosphatases. For instance, a myosin phosphatase counteracts ROCK function and also regulates cytokinesis (Matsumura, 2005; Piekny et al., 2005). In general, however, how protein phosphatases modulate cytoskeletal organization during cell division is incompletely understood.

Ser/Thr protein phosphatases can be placed into one of eight groups based on sequence conservation within the catalytic domain: PP1, PP2A, PP2B, PPP3, PP4, PP5, PP6 or PP7 (reviewed by Moorhead et al., 2009). The PP2A, PP4 and PP6 phosphatases are highly related to one another. PP2A acts as a trimetric holoenzyme, consisting of catalytic (C), structural (A) and regulatory (B) subunits. The presence of different structural and regulatory subunits allows for the combinatorial assembly of a variety of holoenzymes that target distinct substrates, thus generating functional diversity. PP2A phosphatases function in diverse processes, including cell cycle progression, cell growth and apoptosis (reviewed by Bollen et al., 2009; Lechward et al., 2001). In addition, PP2A phosphatases regulate microtubule organization during mitosis (Gliksman et al., 1992; Schlaitz et al., 2007). The phosphatase PP4 similarly functions as a heterotrimeric complex. In addition to a role in chromatin remodeling and DNA repair, PP4 is required for meiotic recombination, cell cycle progression, mitotic spindle assembly and chromosome segregation (reviewed by Cohen et al., 2005; Han et al., 2009; Toyo-oka et al., 2008).

The *Saccharomyces cerevisiae* PP6 ortholog Sit4p regulates G1 progression and TOR signaling, whereas in *Schizosaccharomyces pombe* Ppe1p contributes to chromosome segregation (Goshima et al., 2003; Rohde et al., 2004; Sutton et al., 1991). In mammalian cells, PP6 targets IκBε for degradation in response to TNFα and activates DNA-dependent protein kinase to trigger DNA repair upon ionizing irradiation (Mi et al., 2009; Stefansson and Brautigan, 2006). In yeast and mammalian cells, PP6 proteins associate with

[1]Swiss Institute for Experimental Cancer Research (ISREC), School of Life Sciences, Swiss Federal Institute of Technology (EPFL), Lausanne CH-1015 Switzerland.
[2]Department of Molecular Genetics and Cell Biology, The University of Chicago, Chicago, IL 60637, USA.

*Present address: Northwestern Feinberg School of Medicine, Chicago, IL 60611, USA
†These authors contributed equally to this work
‡Authors for correspondence (mglotzer@uchicago.edu; pierre.gonczy@epfl.ch)

Accepted 6 November 2009

SAPS (Sit4p-associated proteins), which are required for their function (Luke et al., 1996; Stefansson and Brautigan, 2006). Despite substantial progress in recent years in understanding the function of PP6, the potential role of this particular phosphatase during mitosis of metazoan organisms has not been investigated.

The one-cell stage *Caenorhabditis elegans* embryo has proven a powerful experimental system in which to study cell division processes in a developing organism (reviewed by Oegema and Hyman, 2005). First, cell division occurs in a similar manner in nematode embryos as in most animal cells and can be monitored with high resolution using time-lapse microscopy. Second, the large size (~50 μm) of the one-cell stage embryo renders it readily amenable to experimental manipulations. Third, RNA interference (RNAi) is particularly potent for depleting components from early *C. elegans* embryos. Thus, RNAi-based functional genomic screens have led to the identification of many novel components essential for cell division.

The microtubule and the actin cytoskeleton undergo pronounced changes and play important roles in one-cell stage *C. elegans* embryos (reviewed by Cowan and Hyman, 2007; Gönczy, 2008). The sperm-contributed centrosome serves as a symmetry-breaking signal that is thought to locally relax the actomyosin network and to initiate the establishment of anteroposterior (AP) polarity. The cortical actomyosin network then retracts from the embryo posterior, concentrating actin and the non-muscle myosin II NMY-2 in the embryo anterior. The mitotic spindle initially assembles in the cell center, but is displaced thereafter towards the posterior in response to AP polarity cues. Asymmetric spindle positioning follows from an imbalance of net pulling forces acting on the two spindle poles during anaphase (Grill et al., 2001). These pulling forces rely on a ternary complex comprising two partially redundant heterotrimeric G protein alpha subunits, GOA-1 and GPA-16, the essentially identical GoLoco proteins, GPR-1 and GPR-2, as well as the coiled-coil protein LIN-5 (Colombo et al., 2003; Gotta and Ahringer, 2001; Gotta et al., 2003; Nguyen-Ngoc et al., 2007; Srinivasan et al., 2003). The Gα–GPR-1/2–LIN-5 ternary complex is evolutionary conserved and plays a related role in asymmetric cell division in *Drosophila* and spindle positioning in human cells (reviewed by Gönczy, 2008). The available evidence suggests that the complex promotes recruitment of the minus-end directed motor dynein to the cell cortex, which, together with microtubule depolarization, generates pulling forces on astral microtubules. As a result of asymmetric spindle positioning, the cleavage furrow assembles slightly to the posterior and the first cell division is unequal. Despite the identification of components essential for pulling forces and cytokinesis, less is known about how these processes are modulated in time and space. Here, we report that the PP6 phosphatase PPH-6 and its associated subunit SAPS-1 are crucial for modulating cortical contractility and spindle positioning in one-cell stage *C. elegans* embryos.

MATERIALS AND METHODS

Nematodes and RNAi

C. elegans wild-type (N2), *zen-4(or153)* (Severson et al., 2000), *goa-1(sa734)* (Robatzek and Thomas, 2000), *let-99(or204ts)* (Goulding et al., 2007), as well as transgenic lines expressing GFP-NMY-2 and GFP-MOE (Motegi et al., 2006b; Munro et al., 2004) were maintained using standard protocols. The mutant strains were maintained at 16°C and shifted to 24°C for at least 24 hours prior to analysis. For generating transgenic animals expressing GFP-PPH-6 or GFP-SAPS-1, corresponding full-length cDNAs were obtained by RT-PCR (*pph-6*) or from the plasmid yk513G7 (*saps-1*, a gift from Yuji Kohara, National Institute of Genetics, Mishima, Japan) and subcloned into the germline expression vector pSU25 (Bellanger and Gönczy, 2003). Sequence verified constructs were bombarded (Praitis et al., 2001) yielding one integrated line for GFP-SAPS-1 and three lines for GFP-PPH-6, two of which were integrated; the third non-integrated line exhibited stronger expression and was retained for analysis.

Bacterial RNAi feeding strains for *pph-6*, *saps-1* and *csnk-1* were obtained from the *C. elegans* ORFeome RNAi library (gift from Jean-François Rual and Marc Vidal, Harvard Medical School, Boston, USA) and prepared as described (Kamath et al., 2001). RNAi for *gpa-16* was performed as described (Afshar et al., 2004). RNAi for *pph-6* or *saps-1* was performed by feeding L3-L4 animals with bacteria expressing the corresponding dsRNAs at 24°C for 30-36 hours. Combined depletion of SAPS-1 and GPB-1, as well as of SAPS-1 and CSNK-1, or of PPH-6 and SAPS-1, was achieved by feeding L3-L4 animals with bacteria co-expressing dsRNA corresponding to both genes at 24°C for 30-36 hours or 20 hours, respectively. Longer treatment to *saps-1/csnk-1(RNAi)* resulted in sterility, whereas this was not the case after either single RNAi. This synthetic phenotype indicates that double RNAi-mediated inactivation has been effective.

Microscopy and spindle severing

Time-lapse DIC microscopy and dual DIC and fluorescence microscopy were performed as described (Brauchle et al., 2003; Gönczy et al., 1999), using the first signs of nuclear envelope breakdown (NEBD) as t=0. To quantify the extent of cleavage furrow ingression, the distance (d) between the two furrow tips at the time of maximal ingression and the width of the embryo (w) were determined; the extent of ingression was expressed as 1–(d/w).

For Movies 15-17 in the supplementary material, spinning disk microscopy was performed essentially as described (Bellanger and Gönczy, 2003), except that one image was captured on average every 0.4 seconds by stream acquisition. For Movies 11-14 and 18-21 in the supplementary material, images were acquired with a 63×/1.4 NA objective on a Zeiss Axiovert 200M equipped with a Yokogawa CSU-10 spinning disk unit (McBain), illuminated with a 50 mW 473-nm DPSS laser (Cobolt). Images were captured on a Cascade 512B EM-CCD camera (Photometrics), using MetaMorph (Molecular Devices). Movies were subsequently processed using ImageJ and QuickTime for image optimization.

Spindle severing was performed using a Leica LMD microscope equipped with a pulsed N2 laser (λ=337 nM) (Afshar et al., 2004). The spindle was cut either at metaphase, just before the slight posterior shift of the spindle, or at the onset of anaphase. In addition, NEBD was used as a reference point for timing the cuts. Subsequent tracking of spindle poles and measurements of average peak velocities were essentially as described (Grill et al., 2001). In the experiments with Latrunculin A, embryos were bathed in M9 containing 100 μM of the drug in 0.5% DMSO. The intact eggshell protects the embryo from the drug until permeabilization, which was performed with the laser microbeam after rotation of the nucleo-centrosomal complex. Solvent alone did not induce any abnormalities (data not shown).

Antibody production, co-immunoprecipitation and indirect immunofluorescence

PPH-6 antibodies were produced by cloning full-length *pph-6* into pGEX-T1 (Promega), expressing GST-PPH-6 and recovering it in inclusion bodies, which were electrophoresed by SDS-PAGE. The protein was gel purified and injected into a rabbit (Eurogentec). The resulting antibodies were strip-purified against His-PPH-6, and eluted with 0.1 M glycine pH 2.5. Affinity-purified antibodies were dialyzed against PBS and kept at –20°C in 50% glycerol at 0.2 mg/ml.

SAPS-1 antibodies were generated by immunizing two rabbits (PRF&L) with the last 81 amino acids of SAPS-1 fused to GST. Immunopurification did not significantly improve the reactivity, so the SAPS-1 serum was used as such.

LET-99 antibodies were generated by cloning full-length *let-99* into pGEX-T1, expressing GST-LET-99 and recovering it in inclusion bodies, which were electrophoresed by SDS-PAGE. The protein was gel purified and injected into a rabbit (Eurogentec). Strip purification, was performed against GST-LET-99, as described above for PPH-6 antibodies. These antibodies detected a single band of the expected size of ~80 kDa on western

blot of total embryonic lysate and gave rise to the previously reported distribution of LET-99 by indirect immunofluorescence (see Fig. S8G in the supplementary material) (Tsou et al., 2002).

Preparation of embryonic extracts, western blot analysis and immunoprecipitation (using ~5 μg of PPH-6 antibodies and ~3 μg of GFP antibodies) were performed as previously described (Afshar et al., 2004). For western blot analysis, PPH-6 and SAPS-1 antibodies were used at dilutions of 1:1000 and 1:5000, respectively, α-tubulin antibodies at 1:1000. The secondary antibodies, HRP-conjugated goat anti-rabbit or goat anti-mouse (Invitrogen) were used at 1:5000 and 1:1000, respectively.

Embryo fixation and staining for indirect immunofluorescence was performed as described (Gönczy et al., 1999), using 1:200 mouse anti-α-tubulin antibody (DM1A, Sigma), in combination with one of the following antibodies raised in rabbits: 1:100 PPH-6 (this study); 1:500 SAPS-1 (this study); 1:300 LET-99 (this study); 1:200 PAR-2 (Gönczy et al., 2001); 1:5000 PGL-1 (Kawasaki et al., 1998); 1:500 GFP (gift from Viesturs Simanis, EPFL, Lausanne, Switzerland); 1:500 LIN-5 (Nguyen-Ngoc et al., 2007); 1:300 GPR-1/2 (Nguyen-Ngoc et al., 2007); 1:500 GOA-1 (Afshar et al., 2004); 1:500 GPA-16 (Afshar et al., 2005). For immunostaining with GOA-1, GPA-16, LIN-5 and LET-99 antibodies, embryos were fixed in methanol at –20°C overnight and incubated with primary antibodies for one hour at room temperature. For immunostaining with GPR-1/2 antibodies, embryos were fixed in methanol at –20°C for one hour and incubated with primary antibodies overnight at 4°C; these conditions were found to be optimal for revealing a difference in GPR-1/2 distribution between wild-type and *pph-6*(*RNAi*) or *saps-1(RNAi)* embryos. The secondary antibodies Alexa488-conjugated goat anti-mouse (Molecular Probes) and Cy3-conjugated goat anti-rabbit (Dianova) were used at 1:500 and 1:1000, respectively. Slides were counterstained with 1 mg/ml Hoechst 33258 (Sigma) to reveal DNA. Images were collected on an LSM510 Zeiss, LSM710 Zeiss or a SP2 Leica confocal microscope and processed in Adobe Photoshop, maintaining relative intensities within a series.

RESULTS

The PP6 phosphatase PPH-6 functions in early *C. elegans* embryos

During an RNAi-based functional genomic screen (Gönczy et al., 2000), we found that inactivation of the open reading frame (ORF) C34C12.3 results in phenotypes during the pseudocleavage stage and mitosis in one-cell stage *C. elegans* embryos (see below). This ORF encodes the sole catalytic subunit of a PP6 protein phosphatase in the nematode genome and was thus named *pph-6* (*protein phosphatase 6*). Dendogram analysis and sequence alignment confirmed that PPH-6 is a bona fide PP6 family member (Fig. S1 in the supplementary material).

Prominent coordinated rearrangements of the microtubule and cortical actin cytoskeletal networks can be readily visualized in one-cell stage *C. elegans* embryos by time-lapse differential interference contrast (DIC) microscopy. In the wild type, surface cortical contractions are present initially throughout the embryo, but become restricted to the anterior as AP polarity is established (see Movie 1 in the supplementary material). Shortly thereafter, a transient cortical invagination called the pseudocleavage furrow forms near the embryo center (Fig. 1A, –3:30 minutes:seconds, arrowheads). The male and female pronuclei then meet in the embryo posterior before moving towards the center, together with the associated pair of centrosomes, while undergoing a 90° rotation. As a result, the mitotic spindle assembles in the embryo center and along the AP axis (Fig. 1A, 0:00 minutes:seconds; Fig. 1B). During metaphase, the spindle begins moving towards the posterior; this is followed by further posterior displacement during anaphase, accompanied by vigorous transverse oscillations of the posterior spindle pole (Fig. 1A, 4:20-4:30 minutes:seconds; Fig. 1C; see also Movie 2 in the supplementary material). The posterior spindle pole then flattens

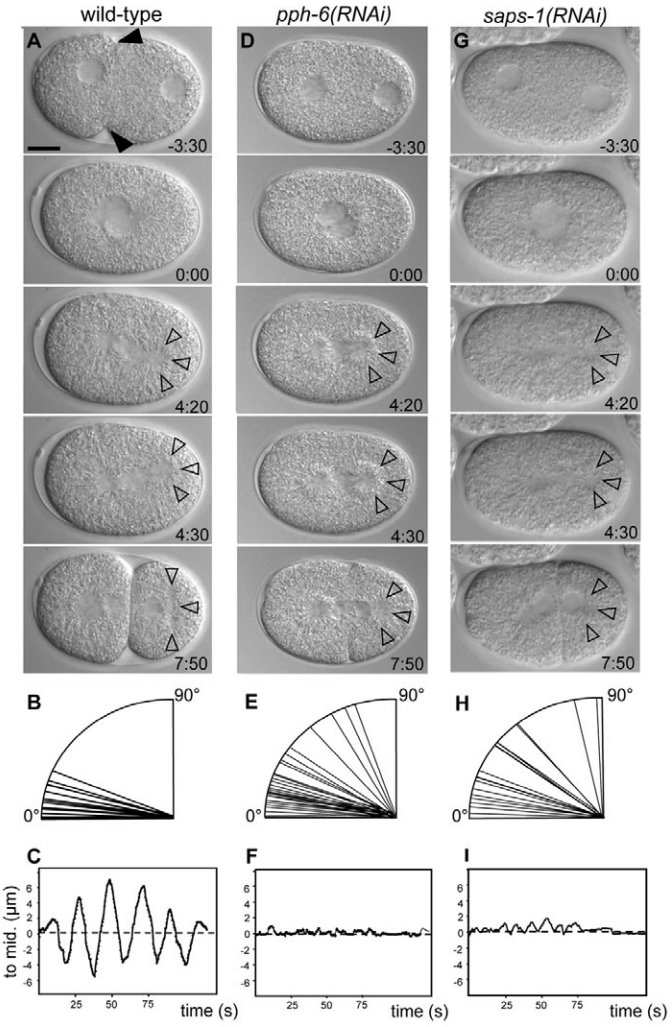

Fig. 1. PPH-6 and SAPS-1 are required for pseudocleavage formation and proper spindle positioning. (**A**,**D**,**G**) Images from DIC time-lapse recordings of wild-type (A), *pph-6(RNAi)* (D) and *saps-1(RNAi)* (G) one-cell stage embryos. Black arrowheads indicate the pseudocleavage furrow; open arrowheads, the posterior spindle pole during anaphase/telophase. Elapsed time is indicated in minutes and seconds (minutes:seconds) with *t*=0 corresponding to nuclear envelope breakdown (NEBD). Unless specified otherwise, scale bars in this and other figures are 10 μm and anterior is to the left. See also corresponding Movies 1, 3 and 5 in the supplementary material. (**B**,**E**,**H**) Representation of the rotation of the nucleo-centrosomal complex (NCC) in wild-type (B), *pph-6(RNAi)* (E) and *saps-1(RNAi)* (H) one-cell stage embryos. Each line represents the axis of the NCC at the time of NEBD in one embryo, with 0° indicating complete rotation onto the AP axis. *n*=25 in each case. (**C**,**F**,**I**) Anaphase posterior spindle pole positions relative to the midline (to mid; +, above; –, below) representative of wild-type (C), *pph-6(RNAi)* (F) and *saps-1(RNAi)* (I) one-cell stage embryos. See also Movies 2, 4 and 6 in the supplementary material.

during telophase and cytokinesis results in the generation of two daughter cells of different sizes, each with a single nucleus containing a complete set of chromosomes (Fig. 1A, 7:50 minutes:seconds).

We found that the sequence of events in one-cell stage *pph-6(RNAi)* embryos differs from that in the wild type (see Movie 3 in the supplementary material). First, whereas small surface cortical contractions are observed initially, they cease rapidly and the

pseudocleavage furrow is absent (Fig. 1D, –3:30 minutes:seconds). Moreover, the two pronuclei meet more centrally than normal and their rotation is sometimes incomplete, such that the mitotic spindle sets up off the AP axis (Fig. 1E). The second prominent phenotype is that although the spindle moves towards the posterior, oscillations of the posterior spindle pole are absent during anaphase and the posterior spindle pole does not flatten during telophase (Fig. 1D, 4:20-7:50 minutes:seconds; Fig. 1F; Movies 3, 4 in the supplementary material). Furthermore, in approximately 15% of *pph-6(RNAi)* embryos (*n*=30), more than one nucleus is present in daughter cells, indicative of partially penetrant defects in chromosome segregation, which were further ascertained using fluorescence time-lapse microscopy of embryos expressing GFP-HistoneH2B and GFP-β-tubulin (data not shown). Accordingly, we found ~17% lethality among the progeny of animals treated with *pph-6(RNAi)* (*n*=101). These results indicate that PPH-6 is essential for proper cortical contractility and spindle positioning in one-cell stage *C. elegans* embryos.

SAPS-1 functions with PPH-6

Given that PP6 phosphatases associate and function with SAPS in other species, we set out to address whether this is the case also in *C. elegans*. We identified a single open reading frame (C47G2.5) that encodes a SAPS protein, which we termed SAPS-1. We found that *saps-1(RNAi)* embryos exhibit indistinguishable phenotypes from those of *pph-6(RNAi)* embryos, including absence of the pseudocleavage furrow and of posterior spindle pole oscillations (Fig. 1G-I; Movies 5, 6 in the supplementary material). We observed an identical phenotype in embryos simultaneously depleted of PPH-6 and SAPS-1 (data not shown).

We raised antibodies against PPH-6 and SAPS-1 to characterize these proteins further. PPH-6 antibodies recognize two species in wild-type embryonic extracts, one major species of the expected size (~37 kDa) and one minor species with a higher molecular weight (Fig. 2A). Both species are specific because they are diminished or absent in *pph-6(RNAi)* embryos (Fig. 2A). The nature of the modification responsible for the higher molecular weight species remains to be investigated. SAPS-1 antibodies recognize two prominent species in wild-type embryonic extracts, with the expected sizes (~ 80 kDa and 87 kDa) of multiple splice variants of SAPS-1 (see www.wormbase.org); both species are depleted in *saps-1(RNAi)* extracts (Fig. 2B). Importantly, co-immunoprecipitation with PPH-6 antibodies established that PPH-6 and SAPS-1 associate in wild-type embryonic extracts (Fig. 2C). We generated a transgenic line expressing GFP-SAPS-1 and found that GFP antibodies co-immunoprecipitate the lower molecular weight species of PPH-6 in extracts derived from such transgenic embryos (Fig. 2D). Moreover, these experiments revealed that PPH-6 and SAPS-1 mutually stabilize each other (Fig. 2C, input lanes).

We next determined the distribution of PPH-6 and SAPS-1 in early *C. elegans* embryos. For PPH-6, we found that the bulk of the signal is cytoplasmic, with some enrichment at microtubule asters (Fig. 3A, arrowheads). These signals are specific, as they are essentially absent in *pph-6(RNAi)* embryos (Fig. 3B). We generated a transgenic line expressing GFP-PPH-6 and found that this fusion protein has an analogous distribution to that of endogenous PPH-6 (see Fig. S2A in the supplementary material). In addition, GFP-PPH-6 was detected at the cell cortex, which was more apparent in two- or four-cell stage embryos, presumably because two cortices from neighboring cells are juxtaposed (see Fig. S2A, arrowhead, in the supplementary material). Closer examination also revealed a weak cortical signal detectable with PPH-6 antibodies (Fig. 3C, arrow). For SAPS-1, we found that the bulk of the signal is also

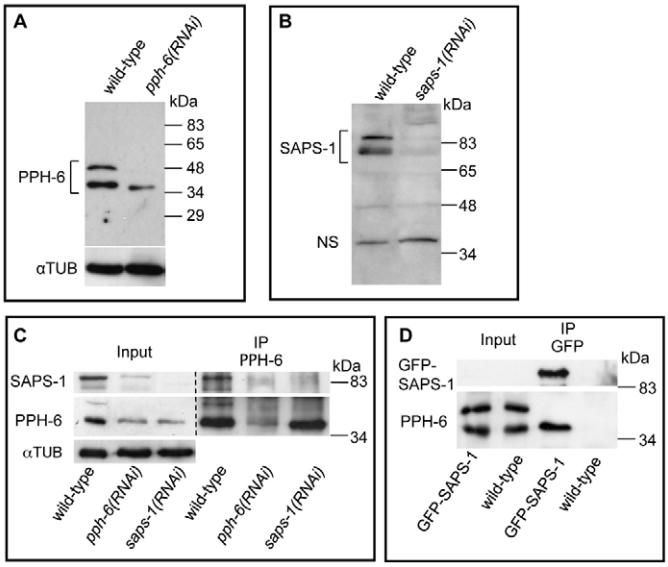

Fig. 2. PPH-6 and SAPS-1 associate in vivo. (**A**) Western blot analysis using PPH-6 antibodies on wild-type or *pph-6(RNAi)* embryonic extracts. The blot was reprobed with α-tubulin antibodies as a loading control (bottom). Note the presence of two species, with the lower one exhibiting the predicted molecular weight of PPH-6 (~37 kDa). Note also that the ratio between these two species varies among extracts (compare A with inputs in C). Similar variability is observed for SAPS-1 (B,C). The variation might be due to differences in the developmental stages of the embryos in the different preparations. (**B**) Western blot analysis of wild-type or *saps-1(RNAi)* embryonic extracts probed with SAPS-1 antibodies. Note presence of two major specific species, exhibiting the predicted molecular weight of the splice variants of SAPS-1 (~80 kDa and 87 kDa). A non-specific band (NS) served as a loading control. (**C**) Coimmunoprecipitation from wild-type, *pph-6(RNAi)* or *saps-1(RNAi)* embryonic extracts using PPH-6 antibodies. Western blots were probed with antibodies against PPH-6, SAPS-1 or α-tubulin, as indicated. In the second row, the input is exposed 10 times longer than the IP. Input/IP=1:50. In three independent experiments, we observed that PPH-6 antibodies retrieved more PPH-6 from the *saps-1(RNAi)* extract than from the *pph-6(RNAi)* extract, despite similar depletion levels of PPH-6. Perhaps PPH-6 not bound to SAPS-1 is more accessible to PPH-6 antibodies. (**D**) Extract from embryos expressing GFP-SAPS-1 or from wild-type embryos immunoprecipitated with GFP antibodies and analyzed by western blot with GFP or PPH-6 antibodies, as indicated. Note that only the PPH-6 species with the lower molecular weight co-immunoprecipitates with GFP-SAPS-1. Input/IP=1:50.

cytoplasmic, with some enrichment at asters and the cell cortex (Fig. 3F-I). We found an analogous distribution for GFP-SAPS-1 (see Fig. S2B in the supplementary material). Moreover, we found that the overall signal intensities of PPH-6 were reduced in *saps-1*(*RNAi*) embryos, and reciprocally in line with the western blot results (Fig. 3E,J; see also Fig. S2C,D in the supplementary material). The fact that PPH-6 and SAPS-1 have overlapping distributions lends further support to the view that they associate in vivo.

Overall, we conclude that PPH-6 exists in a complex with SAPS-1 and that the two components ensure normal protein levels of their partner. For simplicity and unless otherwise indicated, the findings pertaining to the PPH-6–SAPS-1 complex (PPH-6/SAPS-1) are discussed and illustrated hereafter solely for *saps-1(RNAi)* embryos, where the extent of depletion achieved by RNAi is typically more robust, but analogous results were obtained in each instance with *pph-6(RNAi)*.

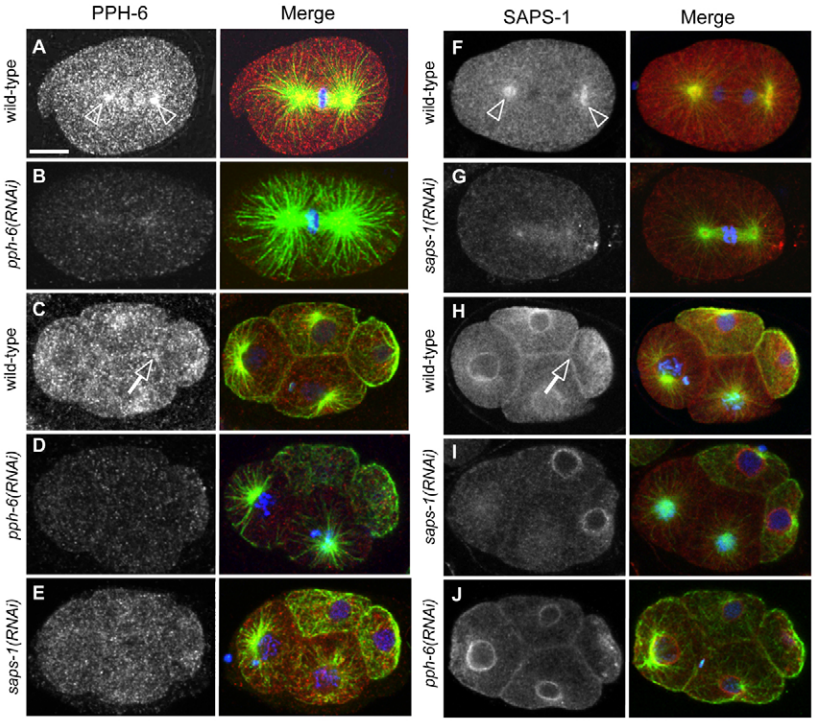

Fig. 3. PPH-6 and SAPS-1 distribution in early embryos. One-cell stage (**A**,**B**,**F**,**G**) or four-cell stage (**C-E**,**H-J**) embryos of the indicated genotypes stained with antibodies against PPH-6 (A-E) or SAPS-1 (F-J), shown alone on the left and in red in the merged panels, as well as against α-tubulin (green in the merged panels); DNA is viewed in blue. Arrowheads in A and F indicate enrichment at microtubule asters; arrows in C and H, enrichment at the cell cortex. Note that the perinuclear signal detected by SAPS-1 antibodies does not appear to be specific, as it is not diminished in *saps-1(RNAi)* embryos (I). Panels E and J are representative of 20 and 17 embryos, respectively, other panels of at least 30 embryos.

PPH-6/SAPS-1 is required for the organization of NMY-2 cortical patches

Given that surface contractions and pseudocleavage formation can result in impaired AP polarity (Kirby et al., 1990; Motegi et al., 2006a; Schonegg and Hyman, 2006), we investigated whether polarity was altered in *saps-1(RNAi)* embryos. We found that the polarity protein PAR-2 and P-granules were distributed normally in *saps-1(RNAi)* one-cell stage embryos (see Fig. S3A-D in the supplementary material). Moreover, live imaging of embryos expressing GFP-PAR-2 or GFP-PAR-6 indicated that severe depletion of PPH-6/SAPS-1 does not result in a discernable effect on the timing of polarity establishment (see Fig. S3E-H and Movies 7-10 in the supplementary material).

The reduced surface contractions in *saps-1(RNAi)* embryos are most suggestive of a defect in the cortical actomyosin network, as observed, for instance, following depletion of the anillin ANI-1 (Maddox et al., 2005). To investigate whether PPH-6/SAPS-1 is required for the integrity of the cortical actomyosin network, we first monitored cortical actin filaments by imaging the actin-binding protein GFP-MOE (Motegi et al., 2006b) using spinning disc confocal microscopy. As illustrated in Fig. 4A,B, as well as by comparing Movies 11 and 12 in the supplementary material, the distribution of GFP-MOE was not markedly altered in *saps-1(RNAi)* embryos during the pseudocleavage stage. In addition, we examined the dynamics of the non-muscle myosin II NMY-2 fused to GFP (Munro et al., 2004). In the wild type, cortical GFP-NMY-2 coalesces into discrete patches during the time of uniform surface contractions; these patches persist and become enriched on the anterior during the pseudocleavage stage (Fig. 4C,E; see also Fig. S4A and Movies 13, 15 in the supplementary material). In *saps-1(RNAi)* embryos, by contrast, we found that whereas GFP-NMY-2 also coalesces into discrete patches initially, these patches are smaller than in wild-type embryos and do not persist during the pseudocleavage stage, so that cortical GFP-NMY-2 disperses rapidly (Fig. 4D,F; see also Fig. S4B, Fig. S5A, and Movies 14, 16 in the supplementary material). This defect is different from that observed in *ani-1(RNAi)* embryos, in which cortical GFP-NMY-2 does not coalesce into patches at all (see Fig. S4C, Movie 17 in the supplementary material) (Maddox et al., 2005), suggesting that PPH-6/SAPS-1 and ANI-1 promote NMY-2 clustering in different manner. Automated analysis of the GFP-NMY-2 foci confirmed that PPH-6/SAPS-1 depletion caused a shift in the intensity profile of myosin foci, with small foci being present, but larger foci being significantly diminished (see Fig. S5A in the supplementary material). Furthermore, we examined the change in relative distance of pairs of GFP-NMY-2 foci over short (10 second) intervals in wild-type and *saps-1(RNAi)* embryos. Whereas, pairs of foci contracted towards each other on average in wild-type embryos, they instead dispersed slightly in *saps-1(RNAi)* embryos (see Fig. S5C in the supplementary material), which likely explains why larger foci do not readily form.

Overall, we conclude that PPH-6/SAPS-1 is required for the maintenance of cortical patches of GFP-NMY-2 during the pseudocleavage stage. Given that NMY-2 is required for actomyosin contractility (Guo and Kemphues, 1996; Munro, 2004), the lack of NMY-2 clustering likely explains the observed defect in pseudocleavage formation in embryos depleted of PPH-6/SAPS-1.

PPH-6/SAPS-1 plays a role during cytokinesis

Although embryos depleted of PPH-6/SAPS-1 are defective in pseudocleavage formation, they do not exhibit cytokinesis defects, even though both processes rely on actomyosin network contraction. To investigate why this might be, we first addressed whether PPH-6/SAPS-1 also plays a role in NMY-2 distribution during anaphase and cytokinesis. In the wild type, large patches of GFP-NMY-2 become apparent at the cell cortex upon anaphase onset and form a contractile network via connecting actin bundles (Fig. 5A; see also Fig. S6C, Movie 18 in the supplementary material). In *saps-1(RNAi)* embryos, we found a dramatic reduction of anaphase cortical GFP-NMY-2 patches (Fig. 5B; see also Fig. S6D, Movie 19 in the

supplementary material). Automated analysis revealed a clear shift in the intensity profile of GFP-NMY-2 foci, with large ones being essentially absent (Fig. S5A in the supplementary material). Furthermore, as observed during pseudocleavage, foci did not contract towards each other in *saps-1(RNAi)* embryos, in contrast to in the wild type (supplementary material Fig. S5C). As is the case during pseudocleavage, the actin network visualized by GFP-MOE did not differ markedly from the wild type in *saps-1(RNAi)* embryos during cytokinesis (see Fig. S4D, Fig. S6A,B, and Movies 20, 21 in the supplementary material). These findings indicate that PPH-6/SAPS-1 promotes cortical myosin contractility that generates foci mobility during anaphase and cytokinesis.

Two genetically redundant pathways control cytokinesis in *C. elegans* embryos. One pathway is regulated by astral microtubules and bears similarities to that involved in pseudocleavage furrow formation, whereas the other requires the central spindle (Bringmann and Hyman, 2005; Dechant and Glotzer, 2003; Werner et al., 2007) (reviewed by Werner and Glotzer, 2008). This prompted us to test whether PPH-6/SAPS-1 is required for cleavage furrow formation in embryos with a compromised central spindle. We combined *saps-1(RNAi)* with a mutant in the centralspindlin component ZEN-4 and examined cleavage furrow ingression with time-lapse DIC microscopy. We found that, whereas all *zen-4(or153)* embryos formed deeply ingressing cleavage furrows (average extent of ingression was 88%) and all *saps-1(RNAi)* embryos divided successfully, doubly compromised embryos only formed shallow furrows and never divided (Fig. 5C-F; see also Movies 22-25 in the supplementary material). We conclude that simultaneous perturbation of PPH-6/SAPS-1 and the central spindle

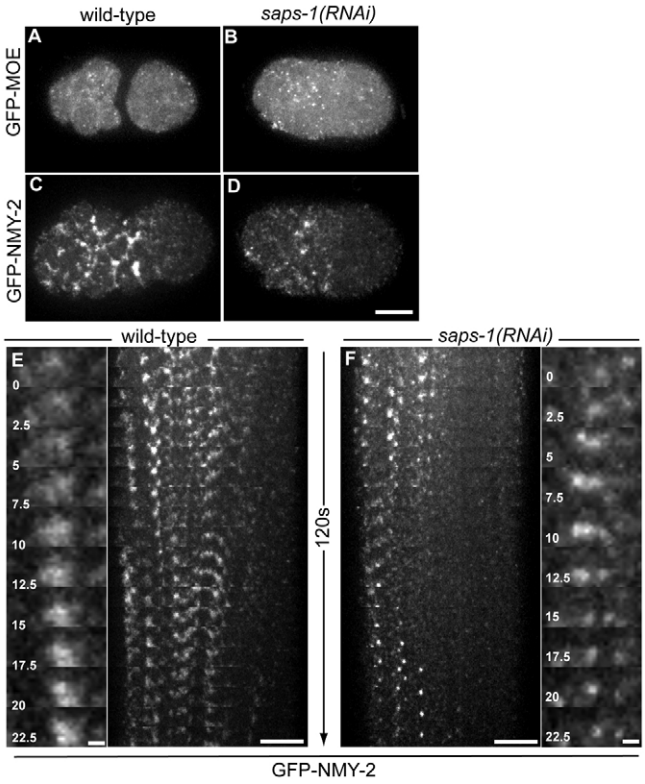

Fig. 4. PPH-6/SAPS-1 is required for clustering of cortical GFP-NMY-2 during pseudocleavage. (**A-D**) Images from spinning disc confocal recordings of the cortex during pseudocleavage of wild-type and *saps-1(RNAi)* embryos expressing GFP-MOE or GFP-NMY-2. Images are representative of at least 10 embryos. See also Movies 11-14 in the supplementary material. Note that quantification of the total GFP-MOE signal was unreliable at this stage because segments of the cortex were out of focus in wild-type embryos owing to cortical invaginations (see center of embryo in A). (**E**,**F**) Kymographs assembled from images acquired two minutes prior to pronuclear meeting of representative recordings of GFP-NMY-2 in wild-type (E) or *saps-1(RNAi)* (F) embryos. Flanking kymographs show a region at high magnification over 22.5 seconds. The bright dots at the bottom of F are new NMY-2 foci that also fail to cluster. Scale bars in the magnified images: 1 μm.

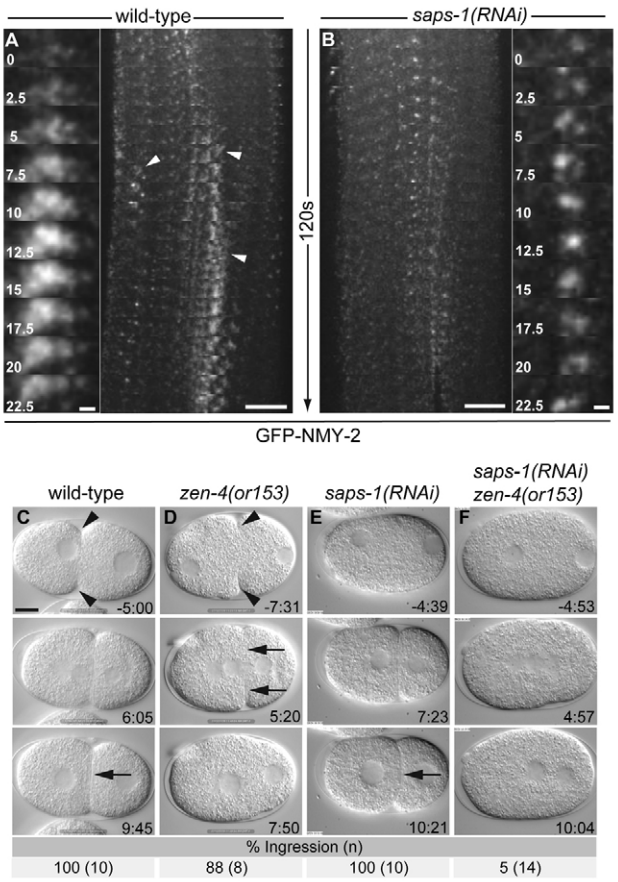

Fig. 5. PPH-6/SAPS-1 plays a role during cytokinesis. (**A**,**B**) Kymographs assembled from images acquired during the first two minutes after anaphase onset of representative recordings of GFP-NMY-2 in wild-type (A) or *saps-1(RNAi)* (B) embryos, representative of 11 embryos each. Arrowheads indicate select foci that intensify in the following frames by the local coalescence of smaller foci. Flanking kymographs show a region at high magnification over 22.5 seconds. Scale bars in the magnified images: 1 μm. (**C-F**) Images from DIC time-lapse microscopy of embryos of the indicated genotypes. Arrowheads indicate the pseudocleavage furrow; arrows, the extent of ingression of the cleavage furrow at end of the first cycle. Elapsed time relative to NEBD is indicated in minutes and seconds (minutes:seconds). See also corresponding Movies 22-25 in the supplementary material. The maximum extent of furrow formation at the end of the first cell cycle, averaged for the indicated number of embryos and rounded to the nearest integer, is shown below the images. Values are expressed in percentages relative to the width of the embryo at the site of furrow formation. Exact values, ±s.d. are as follows: *zen-4(or153)*, 88.5±5.4%; *pph-6(RNAi) zen-4(or153)*, 6.7±4.5%; *saps-1(RNAi)*; *zen-4(or153)*, 5.0±4.9%.

causes a severe defect in furrow formation, indicating that PPH-6/SAPS-1 contributes to cytokinesis by regulating the astral pathway. As the astral pathway relies on contractile properties of the cortical actomyosin network (Werner et al., 2007), the absence of NMY-2 patches in embryos depleted of PPH-6/SAPS-1 explains why the cleavage furrow is perturbed when both PPH-6/SAPS-1 and the central spindle are lacking.

PPH-6/SAPS-1 positively regulates pulling forces during anaphase

We next investigated the basis of the abnormal spindle behavior during anaphase upon PPH-6/SAPS-1 depletion. The absence of posterior spindle pole oscillations and flattening are reminiscent of conditions in which pulling forces are compromised (Afshar et al., 2004; Colombo et al., 2003; Gotta and Ahringer, 2001). To examine whether this is the case in embryos depleted of PPH-6/SAPS-1, we performed spindle-severing experiments in which the movement of the liberated spindle poles provides a readout of the extent of net force pulling on them (Grill et al., 2001). In metaphase, we found that the average peak velocities of the liberated anterior and posterior spindle poles were, respectively, ~0.65 μm/second and ~0.7 μm/second in the wild type and that they were not affected by PPH-6/SAPS-1 depletion (Fig. 6; see also Table S1 in the supplementary material). A strikingly different result was observed during anaphase. In the wild type, the average peak velocities of the anterior and posterior spindle poles were ~0.68 μm/second and ~1.1 μm/second, respectively (Fig. 6) (Afshar et al., 2004; Grill et al., 2001). By contrast, peak velocities in anaphase *saps-1(RNAi)* embryos were only ~0.39 μm/second and ~0.57 μm/second, respectively (Fig. 6; see also Table S1 in the supplementary material). We conclude that PPH-6/SAPS-1 is required for proper pulling forces specifically during anaphase.

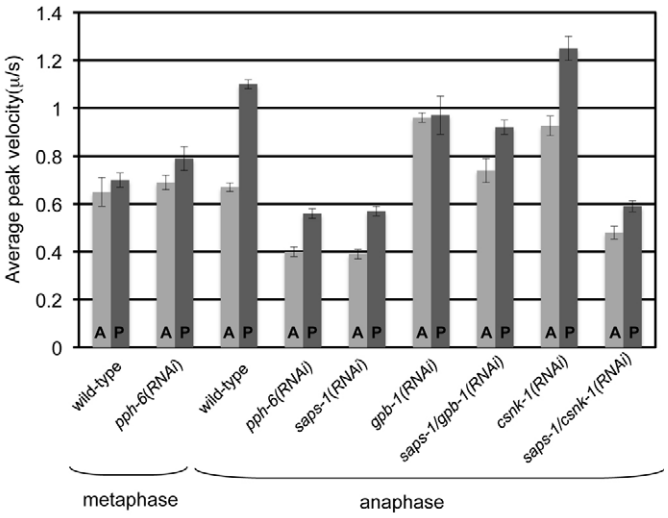

Fig. 6. PPH-6/SAPS-1 promotes pulling forces. Average peak velocities ± s.e.m. of anterior (A) and posterior (P) spindle poles after spindle severing in one-cell stage embryos of the indicated genotypes. Spindle severing was performed during metaphase or early anaphase, as indicated. Actual values and number of embryos analyzed are given in Table S1 in the supplementary material. The values for *gpb-1(RNAi)* are from Afshar et al. (Afshar et al., 2004). The fact that the anterior peak velocity for embryos simultaneously depleted of CSNK-1 and SAPS-1 is slightly higher than that for embryos depleted solely of SAPS-1 might stem from the fact that doubly depleted embryos were analyzed at an earlier time point, as more complete depletion results in sterility.

PPH-6/SAPS-1 promotes cortical GPR-1/2 and LIN-5

We investigated whether the aberrant organization of the anaphase cortical actomyosin network was responsible for the reduced pulling forces observed after PPH-6/SAPS-1 depletion. To this end, we first conducted spindle-severing experiments in *ani-1(RNAi)* embryos in which cortical patches of GFP-NMY-2 are also absent during anaphase (data not shown). We found, however, that the extent of pulling forces during anaphase was not markedly different between wild-type and *ani-1(RNAi)* embryos, and was much higher than in *saps-1(RNAi)* embryos (see Fig. S7A; see also Table S1 in the supplementary material). Therefore, the absence of NMY-2 patches during anaphase does not necessarily result in significantly lower pulling forces. As a second way to test whether relaxation of the cortical actomyosin network could explain the reduced pulling forces upon PPH-6/SAPS-1 depletion, we treated wild-type embryos with the actin depolymerizing drug Latrunculin A (Lat A) prior to spindle severing. As shown in Fig. S7A in the supplementary material, we found that pulling forces on the anterior spindle pole were increased in Lat A-treated embryos. Although Lat A affects actin in a global manner, this result is compatible with modeling studies in which the enrichment of actin on the anterior cortex was proposed to enhance cortical rigidity and thus limit the extent of effective force generation on that side (Kozlowski et al., 2007). Moreover, Lat A also increased pulling forces in *saps-1(RNAi)* embryos (see Fig. S7A; see also Table S1 in the supplementary material). Overall, we conclude that aberrant organization of the anaphase cortical actomyosin network is not responsible for the reduced pulling forces observed after PPH-6/SAPS-1 depletion.

We sought to investigate whether PPH-6/SAPS-1 regulates the distribution of components of the ternary complex (Gα–GPR-1/2–LIN-5) that is crucial for generating pulling forces. As shown in Fig. S8A-D in the supplementary material, we found that the distribution of GOA-1 and GPA-16 are indistinguishable in wild-type and *saps-1(RNAi)* embryos. By contrast, we found that the presence of GPR-1/2 at the cell cortex was diminished in most anaphase/telophase *saps-1(RNAi)* embryos compared with in wild-type embryos (Fig. 7A-D; see also Fig. S9A,B,E in the supplementary material). Similarly, cortical LIN-5 was also diminished compared with the wild type in anaphase/telophase *saps-1(RNAi)* embryos (see Fig. S8E,F; see also Fig. S9C,D,F in the supplementary material). Total protein levels of GPR-1/2 and LIN-5 were not affected in *saps-1(RNAi)* embryos (see Fig. 7; see also Fig. S8 in the supplementary material; data not shown).

We set out to address whether the diminution of cortical GPR-1/2 and LIN-5 was indeed responsible for the diminution of pulling forces in embryos depleted of PPH-6/SAPS-1. If this were the case, then providing an excess of cortical GPR-1/2 and LIN-5 by another means in this background might alleviate the phenotype. Previous work established that depletion of the Gβ protein GPB-1 results in excess cortical GPR-1/2, presumably because depleting GPB-1 enables GOA-1 and GPA-16 to recruit more cortical GPR-1/2 (Afshar et al., 2005; Tsou et al., 2003). Therefore, we simultaneously depleted SAPS-1 and GPB-1 and conducted spindle-severing experiments. As shown in Fig. 6, pulling forces were markedly increased in such embryos compared with in embryos that were merely depleted of PPH-6/SAPS-1. As anticipated, we found also that cortical levels of GPR-1/2 were restored in such doubly depleted embryos (Fig. 7G,H), although not to the extent observed in *gpb-*

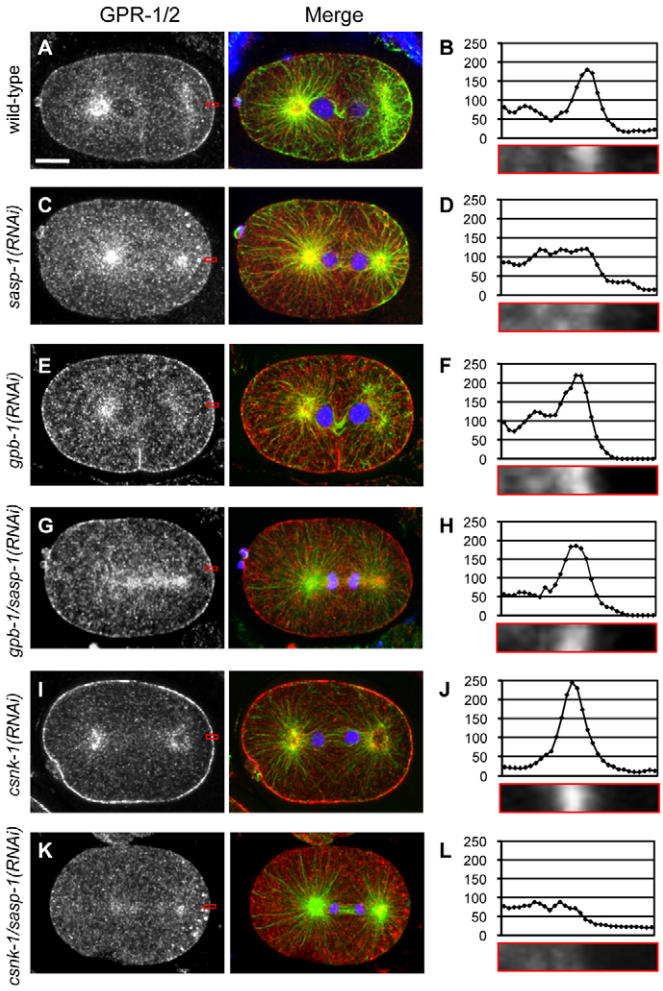

Fig. 7. PPH-6/SAPS-1 contributes to cortical enrichment of GPR-1/2. (**A**,**C**,**E**,**G**,**I**,**K**) Embryos of the indicated genotypes were stained with antibodies against GPR-1/2 (shown alone on the left and in red in the merged panels) and against α-tubulin (green in the merged panels); DNA is viewed in blue in the merged panels. (**B**,**D**,**F**,**H**,**J**,**L**) Quantification of cortical GPR-1/2. A line scan was performed across the 0.7×3.4 μm rectangles depicted in red in the corresponding immunofluorescence panels; the total fluorescence intensity along the horizontal axis of this rectangle is shown in the plots, with the *y*-axis displaying arbitrary gray values. Note that 36% of wild-type embryos (A, *n*=33), 27% of *gpb-1(RNAi)* embryos (E, *n*=20), 20% of *gpb-1/saps-1(RNAi)* embryos (G, *n*=17) and 12% of *csnk-1(RNAi)* embryos (I, *n*=20) exhibited a slightly weaker distribution than that shown. Conversely, 27% of *saps-1(RNAi)* embryos (C, *n*=52) and 10% of *csnk-1/saps-1(RNAi)* embryos exhibited a slightly higher distribution than that shown, yet weaker than in the wild type. See also Fig. S9 in the supplementary material for quantitative analysis.

1(RNAi) (Fig. 7E,F). Together, these findings suggest that PPH-6/SAPS-1 positively regulates pulling forces during anaphase by promoting the cortical localization of GPR-1/2 and LIN-5.

PPH-6/SAPS-1 is required for the excess of pulling forces in LET-99- and CSNK-1-depleted embryos

We considered whether PPH-6/SAPS-1 might exert its function in spindle positioning by regulating LET-99, a DEP-domain containing protein that normally limits cortical GPR-1/2 accumulation on the lateral cortex and thus regulates the pulling forces during centration/rotation and anaphase (Tsou et al., 2002) (see Movie 26 in the supplementary material). We found that the distribution of LET-99 in *saps-1(RNAi)* embryos was identical to that in the wild type (see Fig. S8G,H in the supplementary material). Moreover, spindle behavior and positioning in *let-99(or204ts)* mutant embryos depleted of SAPS-1 resembled that of *saps-1(RNAi)* embryos (see Movie 27 in the supplementary material), together indicating that PPH-6/SAPS-1 does not function by regulating LET-99. We next considered whether there might be a link between PPH-6/SAPS-1 and casein kinase 1 (CSNK-1). CSNK-1 depletion results notably in increased levels of cortical GPR-1/2 and increased pulling forces during anaphase (Panbianco et al., 2008) (Fig. 6, Fig. 7I,J). We found that simultaneous depletion of SAPS-1 and CSNK-1 resulted in levels of cortical GPR-1/2 and of pulling forces that were analogous to those observed in *saps-1(RNAi)* embryos (Fig. 6, Fig. 7K,L). These findings suggest that the modulation of pulling forces by CSNK-1 requires PPH-6/SAPS-1.

DISCUSSION

Compared with the vast knowledge on protein kinases, there is a relative paucity of information regarding the requirement of protein phosphatases for cell division processes. Here, we establish that the protein phosphatase PPH-6 and its associated component SAPS-1 are needed for proper organization of cortical NMY-2 and contractility of the actomyosin network in *C. elegans* embryos. In addition, PPH-6/SAPS-1 contributes to the cortical localization of GPR-1/2 and LIN-5, and to the generation of pulling forces during anaphase.

PPH-6/SAPS-1 is required for a restricted set of processes

We found that depletion of the catalytic subunit PPH-6 by RNAi causes incompletely penetrant defects in chromosome segregation, but penetrant defects in cortical contractility and anaphase pulling forces. Despite these defects, the vast majority of embryos depleted of PPH-6 are viable, in contrast to embryos depleted of the catalytic subunit of PP2A or PP4, suggesting that PPH-6 has a more restricted set of targets in the early embryo. Nevertheless, complete removal of *saps-1* is embryonic lethal (http://www.wormbase.org/db/gene/variation?name=tm2849;class=Variation), indicating that PPH-6 is essential presumably later during embryogenesis. In addition, PPH-6 depletion by RNAi results in slow growth rates and a resistance to Aldicarb, which suggests an additional role for PPH-6 in growth and synaptic transmission (Byrne et al., 2007; Sieburth et al., 2005).

The genome of most eukaryotes contains a multigene family encoding Sit4p-associated proteins (SAPS) that associate and function with PP6 protein phosphatases (Luke et al., 1996). In general, different SAPS exhibit partially overlapping functions, such that their disruption causes a less severe phenotype than does disruption of the catalytic subunit (Luke et al., 1996; Stefansson and Brautigan, 2006). The *C. elegans* genome encodes a single recognizable SAPS protein. As the depletion of SAPS-1 phenocopies the loss of the catalytic subunit, it is likely that all PPH-6 species acting in the early embryo also contain SAPS-1. In human cells, PP6 complexes associate with an additional family of regulators harboring ankyrin repeats. For example, the human SAPS proteins PP6R1 and PP6R3 interact with ankyrin repeat proteins, and such interactions are required for full PP6 activity (Stefansson et al., 2008). Although

there are many uncharacterized ankyrin repeat proteins in *C. elegans*, there is no clear ortholog of those that interact with PP6 in human cells.

The available body of evidence suggests that PPH-6/SAPS-1 independently affects chromosome segregation, cortical contractility and pulling forces. Given that the chromosome segregation defect is partially penetrant, it is unlikely to cause the penetrant defects in cortical contractility and pulling forces. In addition, a lack of cortical contractility precedes chromosome segregation defects. Furthermore, although the motility of NMY-2 aggregates during prophase can be affected by the depletion of Gα proteins (Goulding et al., 2007), cortical contractility and anaphase pulling forces are altered independently of one another in other settings. Thus, embryos depleted of GPA-16 and GOA-1 lack pulling forces but have normal cortical contractility (Colombo et al., 2003; Gotta and Ahringer, 2001). Conversely, we show here that pulling forces are present in embryos depleted of ANI-1, despite a lack of cortical contractility. These considerations lead us to favor the view that PPH-6/SAPS-1 independently regulates chromosome segregation, cortical contractility and pulling forces. It is likely that the phenotypes observed upon depletion of PPH-6/SAPS-1 result from hyperphosphorylation of substrates crucial for each process. Identification of these substrates is an important goal for future investigations.

PPH-6/SAPS-1 regulates cortical contractility and contributes to cytokinesis

An obvious defect following the depletion of PPH-6/SAPS-1 is the lack of a pseudocleavage furrow, which presumably occurs because of the failure of cortical NMY-2 clustering. Although the pseudocleavage furrow does not play an essential role during development (Rose et al., 1995), it reflects the non-uniform activity of the actomyosin network during polarity establishment. Although contractile activity is thought to contribute to the anterior accumulation of PAR-3/PAR-6/PKC-3 (Munro et al., 2004), AP polarity does not appear affected upon depletion of ANI-1 or PPH-6/SAPS-1, which are both essential for robust contractility of the actomyosin network (Maddox et al., 2005) (this study). Therefore, strong contractile activity is not essential to initiate polarity establishment.

There are significant mechanistic similarities between formation of the pseudocleavage furrow and the astral pathway that contributes to cleavage furrow formation during cytokinesis together with the central spindle (Werner et al., 2007). Although cytokinesis can proceed in the absence of PPH-6/SAPS-1, the cleavage furrows have less myosin than in the wild-type and the myosin foci are less contractile, suggesting that cytokinesis is partially compromised. We revealed that this is indeed the case by disrupting the central spindle together with PPH-6/SAPS-1 and observing a near complete block to cleavage furrow ingression. We conclude that PPH-6/SAPS-1 is important for the astral pathway and thus contributes to robust cleavage furrow formation during cytokinesis. One mechanism by which a phosphatase such as PPH-6 could activate NMY-2 is by antagonizing the inhibitory phosphorylation of the myosin phosphatase MEL-11 (Kawano et al., 1999). If this were the sole means by which PPH-6/SAPS-1 regulated myosin, PPH-6 depletion should not have any effect in a *mel-11* mutant in which the cortical network is hyperactive. However, doubly compromised embryos exhibited an intermediate level of contractility (Y.C.T. and M.G., data not shown), suggesting that MEL-11 is not the sole target of PPH-6–SAPS-1 during cytokinesis.

PPH-6/SAPS-1 contributes to anaphase pulling forces

Our analysis uncovered that depletion of PPH-6/SAPS-1 markedly affects pulling forces during anaphase, whereas it has no impact during metaphase. One explanation for this differential requirement is that PPH-6/SAPS-1 acts on the substrate relevant for pulling forces specifically during anaphase. Alternatively, PPH-6/SAPS-1 could function earlier but its absence might only be detectable during anaphase. We favor this second possibility, as PPH-6/SAPS-1 is required for proper rotation of the nucleo-centrosomal complex, just like GPR-1/2 (Park and Rose et al., 2008), indicating that PPH-6/SAPS-1 functions prior to anaphase. In addition, the level of cortical GPR-1/2 is also diminished in *saps-1(RNAi)* embryos earlier in the cell cycle (K.A. and P.G., data not shown). Why would pulling forces not be affected during metaphase in embryos depleted of PPH-6/SAPS-1? One possibility is that pulling forces during metaphase are less sensitive to a diminution of cortical GPR-1/2 than they are during anaphase. Compatible with this view, we found that embryos depleted of either GOA-1 or GPA-16, in which levels of cortical GPR-1/2 are diminished (Afshar et al., 2005), exhibit pulling forces at metaphase that are comparable to those in the wild type (see Fig. S7B in the supplementary material). In addition, gradual depletion of GPR-1/2 first affects anaphase oscillations, whereas only upon further depletion is metaphase spindle displacement affected (Pecreaux et al., 2006). Although under standard experimental conditions the spindle becomes positioned asymmetrically in embryos partially depleted of GPR-1/2 (Pecreaux et al., 2006) or severely depleted of PPH-6/SAPS-1 (this study), it is plausible that this would not be the case under more challenging conditions, for instance at lower temperatures when pulling forces in wild-type embryos are weaker (Johnston et al., 2008).

Our analysis revealed that simultaneous depletion of CSNK-1 and SAPS-1 results in a phenotype similar to that of embryos depleted solely of SAPS-1, both in terms of GPR-1/2 distribution and pulling forces. This finding is consistent with a model in which CSNK-1 somehow acts upon PPH-6/SAPS-1 during spindle positioning. Most likely, CSNK-1 and PPH-6 do not act on the same substrate, because in that case the phenotype of embryos lacking both components should have been similar to that of embryos lacking solely the kinase. We found also that simultaneous depletion of CSNK-1 and SAPS-1 results in severe sterility, as well as a low density of yolk granules (K.A. and P.G., data not shown); these traits are not exhibited following either single depletion, suggesting that CSNK-1 and SAPS-1 might cooperate to regulate several processes. Interestingly, the *S. cerevisiae* casein kinase Hrr25 and the PP6 phosphatase Sit4p also act in the same pathway, in this case to regulate tRNA modification via the Elongator complex (Mehlgarten et al., 2009).

In conclusion, our findings reveal that depletion of PPH-6/SAPS-1 has a profound effect on the contractility of cortical myosin and on the presence of GPR-1/2 and LIN-5 at the cell cortex, thus contributing to the robustness of cell division processes during early development of a metazoan organism.

Acknowledgements

We thank Anthony Hyman, Ed Munro and Fabio Piano for worm strains, Yuji Kohara for an EST clone, Marc Vidal for the RNAi library, Coralie Busso for help in generating transgenic animals, Manuel Kulagin for help with immunostaining, as well as Alexandra Bezler, Marie Delattre and Virginie Hachet for critical reading of the manuscript. Supported by grants from the Swiss National Science Foundation (3100A0-102087 and 3100A0-122500/1 to P.G.) and the NIH (1R01GM085087 to M.G.). Deposited in PMC for release after 12 months.

Competing interests statement
The authors declare no competing financial interests.

Supplementary material
Supplementary material for this article is available at
http://dev.biologists.org/lookup/suppl/doi:10.1242/dev.042754/-/DC1

References

Afshar, K., Willard, F. S., Colombo, K., Johnston, C. A., McCudden, C. R., Siderovski, D. P. and Gönczy, P. (2004). RIC-8 is required for GPR-1/2-dependent Gα function during asymmetric division of *C. elegans* embryos. *Cell* **119**, 219-230.

Afshar, K., Willard, F. S., Colombo, K., Siderovski, D. P. and Gönczy, P. (2005). Cortical localization of the Galpha protein GPA-16 requires RIC-8 function during *C. elegans* asymmetric cell division. *Development* **132**, 4449-4459.

Archambault, V. and Glover, D. M. (2009). Polo-like kinases: conservation and divergence in their functions and regulation. *Nat. Rev. Mol. Cell. Biol.* **10**, 265-275.

Bellanger, J. M. and Gönczy, P. (2003). TAC-1 and ZYG-9 form a complex that promotes microtubule assembly in *C. elegans* embryos. *Curr. Biol.* **13**, 1488-1498.

Bollen, M., Gerlich, D. W. and Lesage, B. (2009). Mitotic phosphatases: from entry to exit guides. *Trends Cell Biol.***10**, 531-541.

Brauchle, M., Baumer, K. and Gönczy, P. (2003). Differential activation of the DNA replication checkpoint contributes to asynchrony of cell division in *C. elegans* embryos. *Curr. Biol.* **13**, 819-827.

Bringmann, H and Hyman, A. A. (2005). A cytokinesis furrow is positioned by two consecutive signals. *Nature* **4**, 731-734.

Byrne, A. B., Weirauch, M. T., Wong, V., Koeva, M., Dixon, S. J., Stuart, J. M. and Roy, P. J. (2007). A global analysis of genetic interactions in *Caenorhabditis elegans*. *J. Biol.* **6**, 8.

Cowan, C. R. and Hyman, A. A. (2007). Acto-myosin reorganization and PAR polarity in *C. elegans*. *Development* **134**, 1035-1043.

Cohen, P. T., Philp, A. and Vazquez-Martin, C. (2005). Protein phosphatase 4 – from obscurity to vital functions. *FEBS Lett.* **579**, 3278-3286.

Colombo, K., Grill, S. W., Kimple, R. J., Willard, F. S., Siderovski, D. P. and Gönczy, P. (2003). Translation of polarity cues into asymmetric spindle positioning in *Caenorhabditis elegans* embryos. *Science* **300**, 1957-1961.

Dechant, R. and Glotzer, M. (2003). Centrosome separation and central spindle assembly act in redundant pathways that regulate microtubule density and trigger cleavage furrow formation. *Dev. Cell* **4**, 333-344.

Gliksman, N. R., Parsons, S. F. and Salmon, E. D. (1992). Okadaic acid induces interphase to mitotic-like microtubule dynamic instability by inactivating rescue. *J. Cell Biol.* **119**, 1271-1276.

Gönczy, P. (2008). Mechanisms of asymmetric cell division: flies and worms pave the way. *Nat. Rev. Mol. Cell. Biol.* **9**, 355-366.

Gönczy, P., Schnabel, H., Kaletta, T., Amores, A. D., Hyman, T. and Schnabel, R. (1999). Dissection of cell division processes in the one cell stage *Caenorhabditis elegans* embryo by mutational analysis. *J. Cell Biol.* **144**, 927-946.

Gönczy, P., Echeverri, G., Oegema, K., Coulson, A., Jones, S. J., Copley, R. R., Duperon, J., Oegema, J., Brehm, M., Cassin, E. et al. (2000). Functional genomic analysis of cell division in *C. elegans* using RNAi of genes on chromosome III. *Nature* **408**, 331-336.

Gönczy, P., Bellanger, J. M., Kirkham, M., Pozniakowski, A., Baumer, K., Phillips, J. B. and Hyman, A. A. (2001). *zyg-8*, a gene required for spindle positioning in *C. elegans*, encodes a doublecortin-related kinase that promotes microtubule assembly. *Dev. Cell* **1**, 363-375.

Goshima, G., Iwasaki, O., Obuse, C. and Yanagida, M. (2003). The role of Ppe1/PP6 phosphatase for equal chromosome segregation in fission yeast kinetochore. *EMBO J.* **22**, 2752-2763.

Gotta, M. and Ahringer, J. (2001). Distinct roles for Galpha and Gbetagamma in regulating spindle position and orientation in *Caenorhabditis elegans* embryos. *Nat. Cell Biol.* **3**, 297-300.

Gotta, M., Dong, Y., Peterson, Y. K., Lanier, S. M. and Ahringer, J. (2003). Asymmetrically distributed *C. elegans* homologs of AGS3/PINS control spindle position in the early embryo. *Curr. Biol.* **13**, 1029-1037.

Goulding, M. B., Canman, J. C., Senning, E. N., Marcus, A. H. and Bowerman, B. (2007). Control of nuclear centration in the C. elegans zygote by receptor-independent Galpha signaling and myosin II. *J. Cell Biol.* **178**, 1177-1191.

Grill, S. W., Gönczy, P., Stelzer, E. H. and Hyman, A. A. (2001). Polarity controls forces governing asymmetric spindle positioning in the *Caenorhabditis elegans* embryo. *Nature* **409**, 630-633.

Guo, S. and Kemphues, K. J. (1996). A non-muscle myosin required for embryonic polarity in *Caenorhabditis elegans*. *Nature* **382**, 455-458.

Han, X., Gomes, J. E., Birmingham, C. L., Pintard, L., Sugimoto, A. and Mains, P. E. (2009). The role of protein phosphatase 4 in regulating microtubule severing in the *Caenorhabditis elegans* embryo. *Genetics* **181**, 933-943.

Johnston, C. A., Afshar, K., Snyder, J. T., Tall, G. G., Gönczy, P., Siderovski, D. P. and Willard, F. S. (2008). Structural determinants underlying the temperature-sensitive nature of a Galpha mutant in *C. elegans* asymmetric cell division. *J. Biol. Chem.* **283**,21550-21558.

Kamath, R. S., Martinez-Campos, M., Zipperlen, P., Fraser, A. G. and Ahringer, J. (2001). Effectiveness of specific RNA-mediated interference through ingested double-stranded RNA in *Caenorhabditis elegans*. *Genome Biol.* **2**, RESEARCH0002.

Kawano, Y., Fukata, Y., Oshiro, N., Amano, M., Nakamura, T., Ito, M., Matsumura, F., Inagaki, M. and Kaibuchi, K. (1999). Phosphorylation of myosin-binding subunit (MBS) of myosin phosphatase by Rho-kinase in vivo. *J. Cell Biol.* **147**, 1023-1038.

Kawasaki, I., Shim, Y. H., Kirchner, J., Kaminker, J., Wood, W. B. and Strome, S. (1998). PGL-1, a predicted RNA-binding component of germ granules, is essential for fertility in *C. elegans*. *Cell* **94**, 635-645.

Kirby, C., Kusch, M. and Kemphues, K. (1990). Mutations in the *par* genes of *Caenorhabditis elegans* affect cytoplasmic reorganization during the first cell cycle. *Dev. Biol.* **142**, 203-215.

Kozlowski, C., Srayko, M. and Nédélec, F. (2007). Cortical microtubule contacts position the spindle in *C. elegans* embryos. *Cell* **129**, 499-510.

Lechward, K., Awotunde, O. S., Swiatek, W. and Muszynska, G. (2001). Protein phosphatase 2A: variety of forms and diversity of functions. *Acta Bioch. Pol.* **48**, 921-933.

Luke, M. M., Della Seta, F., Di Como, C. J., Sugimoto, H., Kobayashi, R. and Arndt, K. T. (1996). The SAP, a new family of proteins, associate and function positively with the SIT4 phosphatase. *Mol. Cell. Biol.* **16**, 2744-2755.

Maddox, A. S., Habermann, B., Desai, A. and Oegema, K. (2005). Distinct roles for two *C. elegans* anillins in the gonad and early embryo. *Development* **132**, 2837-2848.

Matsumura, F. (2005). Regulation of myosin II during cytokinesis in higher eukaryotes. *Trends Cell Biol.* **15**, 371-377.

Mehlgarten, C., Jablonowski, D., Breunig, K. D., Stark, M. J. and Schaffrath, R. (2009). Elongator function depends on antagonistic regulation by casein kinase Hrr25 and protein phosphatase Sit4. *Mol. Microbiol.* **73**, 869-881.

Mi, J., Dziegielewski, J., Bolesta, E., Brautigan, D. L. and Larner, J. M. (2009). Activation of DNA-PK by ionizing radiation is mediated by protein phosphatase 6. *PLoS ONE* **4**, e4395.

Moorhead, G. B., De Wever, V., Templeton, G. and Kerk, D. (2009). Evolution of protein phosphatases in plants and animals. *Biochem. J.* **417**, 401-409.

Motegi, F. and Sugimoto, A. (2006a). Sequential functioning of the ECT-2 RhoGEF, RHO-1 and CDC-42 establishes cell polarity in *Caenorhabditis elegans* embryos. *Nat. Cell Biol.* **8**, 978-985.

Motegi, F., Velarde, N. V., Piano, F. and Sugimoto, A. (2006b). Two phases of astral microtubule activity during cytokinesis in *C. elegans* embryos. *Dev. Cell* **10**, 509-520.

Munro, E., Nance, J. and Priess, J. R. (2004). Cortical flows powered by asymmetrical contraction transport PAR proteins to establish and maintain anterior-posterior polarity in the early *C. elegans* embryo. *Dev. Cell* **7**, 413-424.

Nguyen-Ngoc, T., Afshar, K. and Gönczy, P. (2007). Coupling of cortical dynein and G alpha proteins mediates spindle positioning in *Caenorhabditis elegans*. *Nat. Cell Biol.* **9**, 1294-1302.

Oegema, K. and Hyman, A. (2006). Cell division. *WormBook.* **19**, 1-40. http://www.wormbook.org.

Panbianco, C., Weinkove, D., Zanin, E., Jones, D., Divecha, N., Gotta, M. and Ahringer, J. (2008). A casein kinase 1 and PAR proteins regulate asymmetry of a PIP(2) synthesis enzyme for asymmetric spindle positioning. *Dev. Cell* **15**, 198-208.

Park, D. H. and Rose, L. S. (2008). Dynamic localization of LIN-5 and GPR-1/2 to cortical force generation domains during spindle positioning. *Dev. Biol.* **315**, 42-54.

Pecreaux, J., Roper, J. C., Kruse, K., Julicher, F., Hyman, A. A., Grill, S. W. and Howard, J. (2006). Spindle oscillations during asymmetric cell division require a threshold number of active cortical force generators. *Curr. Biol.* **16**, 2111-2122.

Piekny, A., Werner, M. and Glotzer, M. (2005). Cytokinesis: welcome to the Rho zone. *Trends Cell Biol.* **15**, 651-658.

Praitis, V., Casey, E., Collar, D. and Austin, J. (2001). Creation of low-copy integrated transgenic lines in *Caenorhabditis elegans*. *Genetics* **157**, 1217-1226.

Robatzek, M. and Thomas, J. H. (2000). Calcium/calmodulin-dependent protein kinase II regulates *Caenorhabditis elegans* locomotion in concert with a G(o)/G(q) signaling network. *Genetics* **156**,1069-1082.

Rohde, J. R., Campbell, S., Zurita-Martinez, S. A., Cutler, N. S., Ashe, M. and Cardenas, M. E. (2004). TOR controls transcriptional and translational programs via Sap-Sit4 protein phosphatase signaling effectors. *Mol. Cell. Biol.* **24**, 8332-8341.

Rose, L. S., Lamb, M. L., Hird, S. N. and Kemphues, K. J. (1995). Pseudocleavage is dispensable for polarity and development in *C. elegans* embryos. *Dev. Biol.* **168**, 479-489.

Sbalzarini, I. F. and Koumoutsakos, P. (2005). Feature point tracking and trajectory analysis for video imaging in cell biology. *J. Struct. Biol.* **151**, 182-195.

Schlaitz, A. L., Srayko, M., Dammermann, A., Quintin, S., Wielsch, N., MacLeod, I., de Robillard, Q., Zinke, A., Yates, J. R., 3rd, Muller-Reichert, T., Shevchenko, A., Oegema, K. and Hyman, A. A. (2007). The *C. elegans* RSA complex localizes protein phosphatase 2A to centrosomes and regulates mitotic spindle assembly. *Cell* **128**, 115-127.

Schonegg, S. and Hyman, A. A. (2006). CDC-42 and RHO-1 coordinate acto-myosin contractility and PAR protein localization during polarity establishment in *C. elegans* embryos. *Development* **133**, 3507-3516.

Severson, A. F., Hamill, D. R., Carter, J. C., Schumacher, J. and Bowerman, B. (2000). The aurora-related kinase AIR-2 recruits ZEN-4/CeMKLP1 to the mitotic spindle at metaphase and is required for cytokinesis. *Curr. Biol.* **10**, 1162-1171.

Sieburth, D., Ch'ng, Q., Dybbs, M., Tavazoie, M., Kennedy, S., Wang, D., Dupuy, D., Rual, J. F., Hill, D. E., Vidal, M., Ruvkun, G. and Kaplan, J. M. (2005). Systematic analysis of genes required for synapse structure and function. *Nature* **436**, 510-517.

Srinivasan, D. G., Fisk, R. M., Xu, H. and van den Heuvel, S. (2003). A complex of LIN-5 and GPR proteins regulates G protein signaling and spindle function in *C elegans*. *Genes Dev.* **17**, 1225-1239.

Stefansson, B. and Brautigan, D. L. (2006). Protein phosphatase 6 subunit with conserved Sit4-associated protein domain targets IκBε. *J. Biol. Chem.* **281**, 22624-22634.

Stefansson, B., Ohama, T., Daugherty, A. E. and Brautigan, D. L. (2008). Protein phosphatase 6 regulatory subunits composed of ankyrin repeat domains. *Biochemistry* **47**, 1442-1451.

Sutton, A., Immanuel, D. and Arndt, K. T. (1991). The SIT4 protein phosphatase functions in late G1 for progression into S phase. *Mol. Cell. Biol.* **11**, 2133-2148.

Taylor, S. and Peters, J. M. (2008). Polo and Aurora kinases: lessons derived from chemical biology. *Curr. Opin. Cell Biol.* **20**, 77-84.

Thompson, J. D., Higgins, D. G. and Gibson, T. J. (1994). CLUSTAL W: improving the sensitivity of progressive multiple sequence alignment through sequence weighting, position-specific gap penalties and weight matrix choice. *Nucleic Acids Res.* **22**, 4673-4680.

Toyo-oka, K., Mori, D., Yano, Y., Shiota, M., Iwao, H., Goto, H., Inagaki, M., Hiraiwa, N., Muramatsu, M., Wynshaw-Boris, A., Yoshiki, A. and Hirotsune, S. (2008). Protein phosphatase 4 catalytic subunit regulates Cdk1 activity and microtubule organization via NDEL1 dephosphorylation. *J. Cell Biol.* **180**, 1133-1147.

Tsou, M. F., Hayashi, A., DeBella, L. R., McGrath, G. and Rose, L. S. (2002). LET-99 determines spindle position and is asymmetrically enriched in response to PAR polarity cues in *C. elegans* embryos. *Development* **19**, 4469-4481.

Tsou, M. F., Hayashi, A. and Rose, L. S. (2003). LET-99 opposes Gα/GPR signaling to generate asymmetry for spindle positioning in response to PAR and MES-1/SRC-1 signaling. *Development* **23**, 5717-5730.

Werner, M. and Glotzer, M. (2008). Control of cortical contractility during cytokinesis. *Biochem. Soc. Trans.* **36**, 371-377.

Werner, M., Munro, E. and Glotzer, M. (2007). Astral signals spatially bias cortical myosin recruitment to break symmetry and promote cytokinesis. *Curr. Biol.* **17**, 1286-1297.